Assessing time-of-flight signal-to-noise ratio gains within the myocardium and subsequent reductions in administered activity in cardiac PET studies

Ian S. Armstrong, PhD,[a] Christine M. Tonge, MSc,[a] and Parthiban Arumugam, MD[a]

[a] Nuclear Medicine, Central Manchester University Hospitals, Manchester, UK

Received Apr 13, 2017; accepted Apr 20, 2017
doi:10.1007/s12350-017-0916-x

Background. **Time-of-flight (TOF) is known to increase signal-to-noise ratio (SNR) and facilitate reductions in administered activity. Established measures of SNR gain are derived from areas of uniform uptake, which is not applicable to the heterogeneous uptake in cardiac PET images using fluoro-deoxyglucose (FDG). This study aimed to develop a technique to quantify SNR gains within the myocardium due to TOF.**

Methods. **Reference TOF SNR gains were measured in 88 FDG oncology patients. Phantom data were used to translate reference SNR gains and validate a method of quantifying SNR gains within the myocardium from parametric images produced from multiple replicate images. This technique was applied to 13 FDG cardiac viability patients.**

Results. **Reference TOF SNR gains of +23% ± 8.5% were measured in oncology patients. Measurements of SNR gain from the phantom data were in agreement and showed the parametric image technique to be sufficiently robust. SNR gains within the myocardium in the viability patients were +21% ± 2.8%.**

Conclusion. **A method to quantify SNR gains from TOF within the myocardium has been developed and evaluated. SNR gains within the myocardium are comparable to those observed by established methods. This allows guidance for protocol optimization for TOF systems in cardiac PET. (J Nucl Cardiol 2019;26:405–12.)**

Key Words: Myocardial perfusion imaging: PET • image reconstruction • basic science • PET/CT imaging • image quality

Abbreviations			
BMI	Body mass index	SNR	Signal-to-noise ratio
FDG	Fluoro-deoxyglucose	TOF	Time-of-flight
PET	Positron Emission Tomography		

See related editorial, pp. 413–416

INTRODUCTION

Positron emission tomography (PET) with time-of-flight (TOF) has been commercially available for a

Electronic supplementary material The online version of this article (doi:10.1007/s12350-017-0916-x) contains supplementary material, which is available to authorized users.

The authors of this article have provided a PowerPoint file, available for download at SpringerLink, which summarizes the contents of the paper and is free for re-use at meetings and presentations. Search for the article DOI on SpringerLink.com.

Reprint requests: Ian S. Armstrong, PhD, Nuclear Medicine, Central Manchester University Hospitals, Oxford Road, Manchester, M13 9WL, UK; *Ian.Armstrong@cmft.nhs.uk*

1071-3581/$34.00

decade.[1,2] The primary advantage associated with TOF is an increase of the signal-to-noise ratio (SNR) in the reconstructed images.[3] This increase in SNR, which is manifested as a reduction in image noise, has been used in fluoro-deoxyglucose (FDG) oncology images to increase lesion detection[4] and also permit reductions in administered activity or scan time.[5,6]

There are few studies that have attempted to specifically assess the impact of TOF in cardiac PET. Two studies have evaluated TOF from the perspective of quantification. The first was in rubidium-82 cardiac PET imaging, which showed that TOF increased the rate of reconstruction convergence in very obese patients, with BMI ranging from 36 to 76 kg/m^2.[7] The study observed greater uniformity of myocardial uptake after several reconstruction iterations with TOF due to the improved convergence. Conversely, the second study from the same institution compared myocardial segmental uptake of FDG in oncology patients in non-TOF and TOF images and reported no significant differences in uptake as a result of the two reconstructions.[8] However, this latter study had a study population with considerably lower BMI (ranging from 18.8 to 34.0 kg/m^2), which may explain the difference in findings.

The theory describing the SNR gains associated with TOF PET was established over 30 years ago. It states that SNR increases with an increasing object size and therefore suggests that TOF will be most beneficial in high-body mass index (BMI) patients.[3] The theoretical model was developed with filtered back-projection reconstruction algorithms for a uniform cylindrical object and an ideal top-hat function for the timing resolution. In reality, reconstruction is almost exclusively iterative reconstruction, activity distribution is not uniform in patients, particularly in cardiac studies, and the timing resolution is Gaussian.[9] As a result, the SNR gains observed in FDG oncology images are more modest and may vary depending on the area of the body.[10,11]

In FDG oncology PET images, SNR measured within the liver is a common metric that has been used to quantify image quality.[12] This measurement of SNR is obtained from defining a large region of interest within the liver and calculating the mean voxel value divided by the standard deviation of the voxel values within a region of interest. It requires the area of tracer distribution to be homogeneous, which is relatively common in FDG oncology images. This measurement has been used to evaluate SNR gains from TOF in oncology.[10] Conversely, assessing SNR in heterogeneous distributions such as FDG cardiac PET presents more of a challenge compared with this method. One cannot simply measure the voxel standard deviation within the myocardium as the dominant component of the standard deviation will be the inherent heterogeneity of the tracer distribution itself.

To date, we believe that there are no studies that have attempted to quantify the gain in SNR within the myocardium as a result of TOF to mirror the many studies in oncology imaging. The development of the fluorine-18-based myocardial perfusion agent Flurpiridaz[13,14] combined with the need to reduce nuclear cardiology patient radiation doses as outlined by the American Society of Nuclear Cardiology Position Statement[15] and elsewhere[16] has made this more pertinent. Therefore, there is a need to assess and make use of the potential SNR gains from TOF in cardiac PET to allow further reductions in administered activity for TOF-capable PET systems.

The aim of this work is to develop and evaluate a means of quantifying the gains in SNR due to TOF within the myocardium. This would be used to aid the optimization of dose protocols for TOF systems with fluorine-18 cardiac tracers.

MATERIALS AND METHOD

PET/CT Scanner

All image acquisitions in this study were performed on a Siemens Biograph mCT (Siemens Healthcare, Knoxville, TN) with 64-slice CT and an extended PET axial field of view of 21.6 cm (TrueV option). The TOF timing resolution for the system is quoted as 530 ps.[17] Images were reconstructed without TOF using three iterations and 24 subsets and with TOF using 2 iterations and 21 subsets. It is noted that the number of image updates is different in the TOF and non-TOF reconstructions, with the number for TOF subsets being fixed at 21. Evidence suggests that TOF requires fewer image updates to achieve comparable activity concentration recovery.[6,11,17] Local validation work from oncology studies has determined that this choice of TOF and non-TOF reconstruction parameters yields equivalent quantification. These same TOF and non-TOF parameters were used in the study by Oldan et al.[8] where myocardial uptake was seen to be comparable. Hence, we believe that there should be no impact on interpretation and merely a reduction in image noise in the TOF images. Two sets of voxel dimensions were chosen to correspond to local protocols for oncology and cardiac imaging. These were 4.0 mm in both the transaxial and axial directions for the oncology protocol and 3.2 mm in the transaxial and 2.0 mm in the axial direction for the cardiac protocol. All images were corrected for attenuation and scatter.

Reference SNR Gain

SNR gains from TOF will be related to the timing resolution of the scanner, the implementation of the algorithm by the manufacturer, and the iterative reconstruction parameters that are used locally. Other centers may already have an appreciation for SNR gains based on oncology images. Therefore, we feel that it is useful to include a reference measurement of TOF SNR gain at our institution to demonstrate locally observed SNR gains and whether any gains

observed in cardiac images are comparable. For this, we retrospectively reviewed 88 routine FDG oncology patients. The median [inter-quartile range (IQR)] for patient weight was 72 [62 to 82] kg and the median [IQR] BMI was 26.1 [22.6 to 29.2] kg/m^2. SNR was measured using a 3.0-cm spherical region placed in the right lobe of the liver ensuring that FDG distribution was homogeneous.[12] SNR was calculated as the mean voxel value divided by the voxel standard deviation within the region and will be referred to as SNR_{liver}. The gain in SNR was defined as

$$SNRgain = \frac{(SNR_{TOF} - SNR_{non-TOF})}{SNR_{non-TOF}}.$$

Cardiac Phantom Assessment

A phantom investigation was used to translate the results of the reference SNR gains from oncology images to cardiac images. An anthropomorphic torso phantom with cardiac insert (Data Spectrum, Hillsborough, NC) was used in this study. The phantom was filled with FDG with a nominal cardiac:background activity concentration ratio of 5:1. A 10-minute listmode scan was acquired with dynamic images of various frame lengths and numbers being produced with details to follow. TOF and non-TOF images were reconstructed using the same numbers of iterations as for the oncology data.

Background SNR. To mirror the measurements in the oncology data, the SNR was measured in the uniform background region of the torso phantom on images using the oncology voxel dimensions. Twelve circular regions of 37 mm diameter were drawn on three transaxial slices. SNR was defined as the mean voxel value divided by the voxel standard deviation within each region, which was averaged across the 36 regions and will be referred to as SNR_{BG}.

Measuring SNR in the Myocardium. The method of assessing SNR within the cardiac insert was based on the technique of generating parametric images from multiple replicate images demonstrated by Schmidtlein et al.[18] This technique was used to assess noise in areas of heterogeneous uptake such as malignant lesions. In our study, mean and standard deviation parametric images were generated from the replicate images such that a voxel value represented the mean and standard deviation, respectively, of that particular voxel over the replicate images. From here, a SNR parametric image was produced by dividing the voxel values of the mean image by the voxel values of the standard deviation image on a voxel-by-voxel basis. A mask region was generated by a threshold of the mean image to a percentage of the maximum voxel value within the cardiac insert. The percentage threshold was set manually following visual inspection of the mask on each transaxial slice through the cardiac insert. This mask was transposed onto the SNR image and the mean value of voxels within the mask on the SNR image was calculated and will be referred to as SNR_{myo}. Analysis was performed only on the image volume that contained the cardiac insert. This was to avoid inclusion of high levels of extra-cardiac activity that were expected to be observed in the clinical images. Figure 1 shows a schematic of how the parametric images were produced. The replicate images used here were those with the cardiac protocol voxel dimensions.

The method by Schmidtlein et al. used an external ECG trigger to create the replicate images via a gated reconstruction. This would not be possible in the clinical part of this study due to the necessity to acquire and produce myocardial gated images using an ECG signal from the patient. Therefore, replicate images were generated by a dynamic reconstruction. To assess the robustness of the technique, mean, standard deviation, and SNR parametric images were generated from a variety of total replicate images and frame lengths; these were 5, 10, 15, and 20 images with frame times of 20 and 30 seconds giving a total of eight measurements of the gain in SNR_{myo} due to TOF.

Gain of SNR in Myocardial Viability Patients

Dynamic images consisting of ten 30-second frames were reconstructed retrospectively from 13 patients that were referred for assessment of myocardial viability with FDG. All patient data were fully anonymized prior to inclusion in this work. According to our institution's research board protocol, this evaluation did not require ethical approval or consent. The group included four female patients, the median [IQR] weight was 80 [58 to 95] kg, and the median [IQR] BMI was 27.2 [22.7 to 31.0] kg/m^2. All patients fasted for six hours prior to the administration of 280 MBq (7.6 mCi) of FDG after ensuring that the patient blood glucose level was between 5.5 and 7.7 mmol/ml. A single bed position image was acquired in listmode sixty minutes after the FDG injection. Images were reconstructed with and without TOF as with the phantom study using the cardiac protocol voxel dimensions. SNR parametric images were generated using the technique described in the previous section and the SNR_{myo} was calculated for each patient in the TOF and non-TOF images. As with the phantom data, image analysis was performed only on the image volume that contained the left ventricle. The masked region applied to the SNR image was visually inspected on all transaxial slices through the left ventricle for every patient and was adjusted if necessary to include only the myocardial area.

Statistical Analysis

Continuous data were assessed for normality using a Shapiro-Wilk test. Normally distributed data are expressed as mean and standard deviation. An unpaired *t* test was performed to compare gains in SNR due to TOF in the oncology study group and the cardiac study group. Statistical analysis was performed in StatsDirect v2.7.8 (StatsDirect Statistical Analysis Software, Altrincham, UK).

RESULTS

Reference SNR Gains

Figure 2 shows the reference gain in SNR_{liver} in the oncology patients plotted against patient weight and BMI. The mean and standard deviation of the gain in SNR_{liver} due to TOF were +23% and 8.5%, respectively,

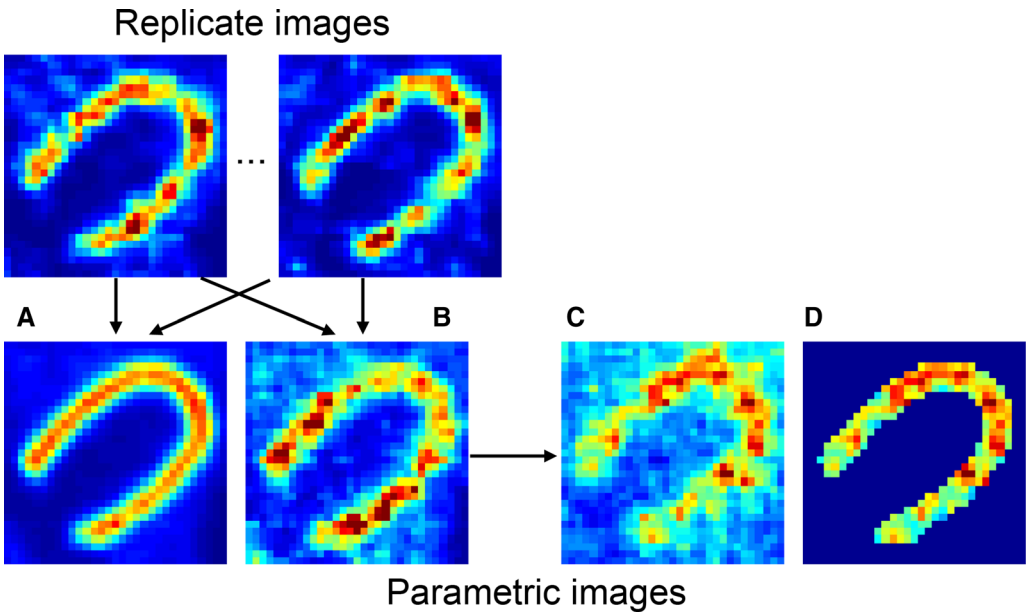

Figure 1. A schematic to show the parametric mean image **A**, standard deviation image **B**, SNR image **C**, and masked SNR image **D** that were created from multiple replicate images. The SNR_{myo} was calculated from the mean of voxels within the masked region as shown in **D**. Data shown are single transaxial slices but analysis was performed over the entire volume of the cardiac insert.

and it can be seen that there is no correlation with patient size.

Cardiac Phantom Assessment

The mean and standard deviation of the gain in SNR_{BG} due to TOF were +21% and 1.6%, respectively, with these values calculated across the 36 regions. This is in good agreement with the measurements of SNR_{liver} gain from the oncology patients. Table 1 shows the gain in SNR_{myo} measured in the phantom cardiac insert derived from the parametric images for the various combinations of number of replicate images and frame length. The mean and standard deviation of the gain in SNR_{myo} due to TOF, across the combinations of replicate images and frame time, were +21% and 0.9%, respectively.

Gain of SNR in Myocardial Viability Patients

Figure 3 shows example parametric masked SNR images from three patients for images reconstructed with and without TOF. Table 2 shows the SNR_{myo} for the non-TOF and TOF images and resultant gain due to TOF for each patient. The mean and standard deviation of the gain in SNR_{myo} due to TOF were +21% and 2.8%, respectively. No statistically significant difference was observed between the measurements of SNR gain compared with those measured in the oncology patients. Figure 4 shows the gain in SNR_{myo} plotted against patient weight and BMI.

DISCUSSION

This study has developed a technique to quantify SNR within the myocardium uptake for FDG. This has allowed the gains in SNR due to TOF to be quantified. Results have been compared with SNR gains measured in clinical FDG oncology images that were acquired according to our local protocol. Phantom data were used to translate the reference SNR gains to the proposed measurement technique within the myocardium. We believe that this is the first study that has attempted to quantify SNR gains within the myocardium arising from TOF in FDG cardiac PET. These findings can be used to guide optimization for imaging protocols and in particular potential reductions in administered activity. The SNR gain can be considered equivalent to a gain in acquired counts comparable to the squared value of SNR gain.[9] Consequently, the findings here suggest that there is an effective gain in acquired counts of close to 50%, which should allow for an approximate reduction of 25% in the administered activity.

The phantom investigation was used to validate the method of assessing the SNR gain within the myocardium. Excellent agreement was observed between the

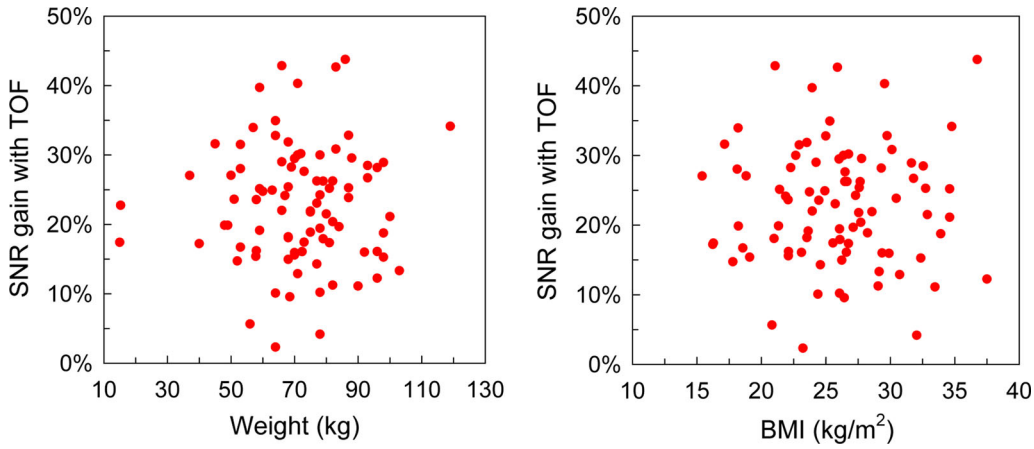

Figure 2. Gain in SNR_{liver} from TOF measured in 88 patients used as a reference for assessing gains in cardiac SNR_{myo}.

Table 1. Gain in SNR_{myo} due to TOF measured in the phantom cardiac insert derived from the parametric images for the various combinations of number of replicate images and frame length

	Frame time (s)	
Number of images	**20 (%)**	**30 (%)**
5	+21	+23
10	+21	+22
15	+21	+21
20	+20	+21

SNR_{BG} gains in the phantom and SNR_{myo} in the phantom cardiac insert derived from parametric images. The range of replicate images and frame time also suggested that the technique was robust across a range of image noise.

Scanner technology continues to advance with PET/MR and now PET/CT systems available with solid-state silicone photomultipliers that offer substantial gains in TOF performance compared with the current generation of TOF systems with photomultipliers.[19] These systems are already demonstrating potential for substantial reductions in radiation dose in oncology imaging.[20] The methods proposed will be useful in assessing the benefits in cardiac PET.

Study Limitations

The primary limitation of this study is the relatively small number of clinical cardiac cases that have been included. However, we believe that when combined with the validation data from the phantom investigation, there are sufficient data to illustrate the benefits of TOF. The second limitation is that the parametric image technique that has been evaluated is applicable only to cardiac PET studies where the tracer distribution over the timescale of image acquisition is fixed. This inhibits the use of the technique in rubidium-82 cardiac PET due to the very short half-life of the tracer. However, we believe that it is a fair assumption that similar SNR gains would be observed with TOF for static and gated rubidium-82 cardiac images. With the future prospect of fluorine-18-based perfusion tracers, the method can be further utilized. Finally, this work demonstrates the SNR gains only for a static image, but we believe that the SNR gains should translate into ECG-gated images as well.

NEW KNOWLEDGE GAINED

A technique of assessing SNR gains due to TOF within the myocardium has been developed and the results compared against gains observed in oncology studies using a translational phantom experiment. The magnitude of gains in SNR within the myocardium is comparable to those measured in oncology patients that have been measured using established techniques. While we have used the technique to assess gains with TOF, the method could be equally applicable to other forms of optimization in cardiac PET such as evaluating a weight-based dosing protocol.

CONCLUSION

A technique of assessing SNR gains due to TOF within the myocardium has been developed for cardiac PET using fluorine-18 tracers. TOF offers gains in SNR for tracer distribution within the myocardium comparable to those observed in oncology imaging on a like-for-like PET/CT system. Based on the TOF performance of

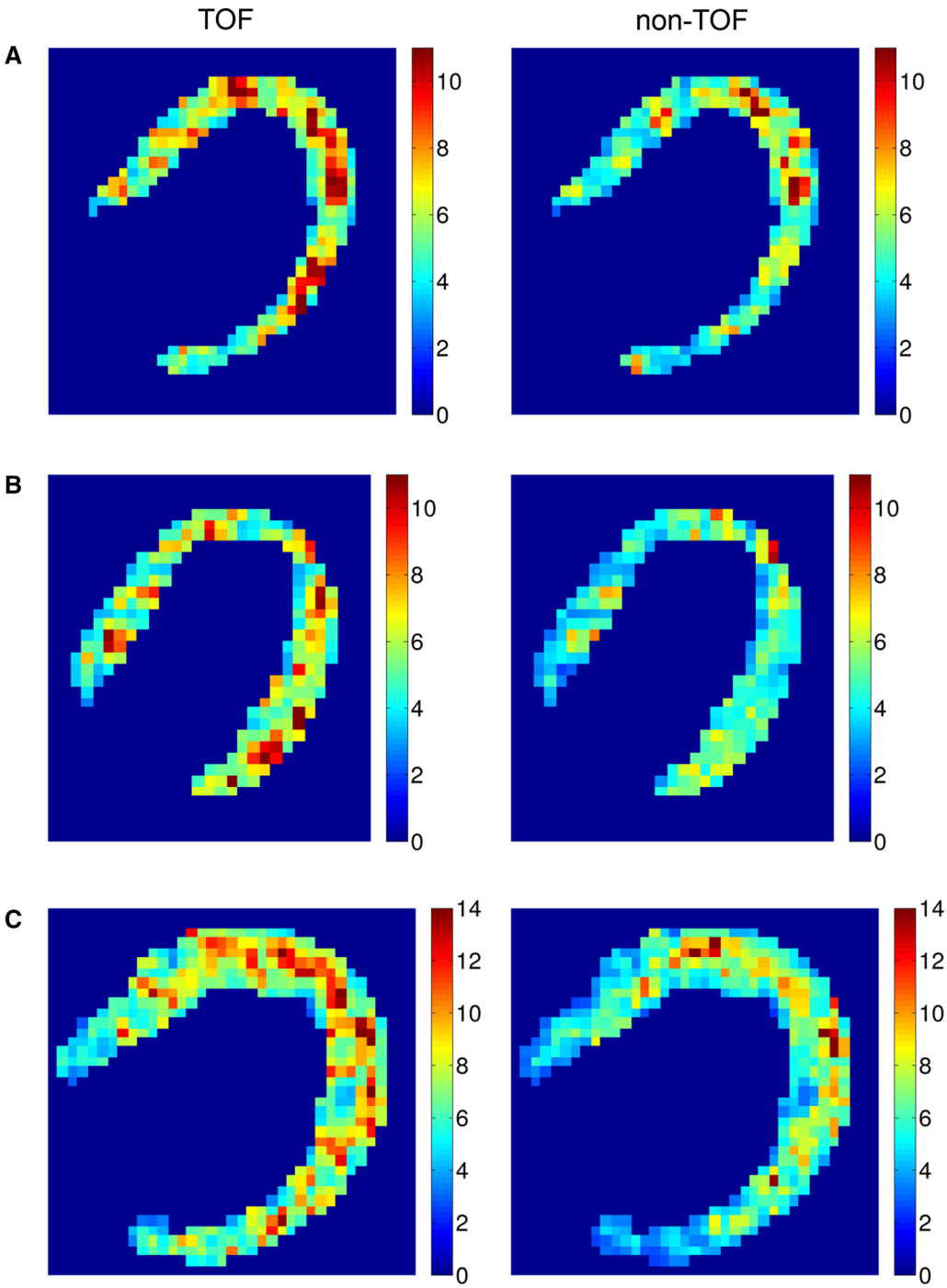

Figure 3. Single transaxial slices from masked SNR parametric images for **A** a female patient with weight 82 kg and BMI 34.6 kg/m^2, **B** a female patient with weight 58 kg and BMI 22.7 kg/m^2, and **C** a male patient with weight 67 kg and BMI 25.5 kg/m^2. Note that the color scale is fixed for pairs of TOF and non-TOF images from the same corresponding patient.

Table 2. SNR_{myo} in the myocardium for non-TOF and TOF images and resultant gain in SNR calculated from the parametric images for the 13 patients referred for cardiac viability imaging

Gender	BMI (kg/m^2)	non-TOF SNR_{myo}	TOF SNR_{myo}	Gain in SNR_{myo} (%)
F	21.5	5.0	6.1	+22
F	34.6	4.8	5.8	+22
F	22.7	4.0	4.9	+23
M	34.0	2.7	3.3	+25
M	25.5	4.9	6.0	+22
M	28.9	3.5	4.0	+15
M	17.0	4.5	5.5	+20
M	37.7	1.6	1.8	+17
M	27.2	3.1	3.7	+20
M	26.1	2.8	3.4	+21
M	28.0	3.1	3.8	+21
M	31.0	2.5	3.1	+24
F	22.4	3.9	4.8	+22

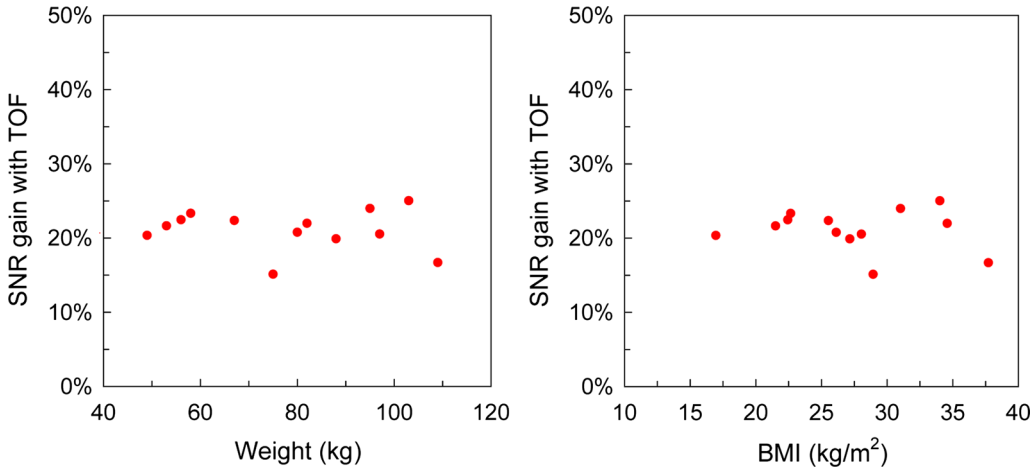

Figure 4. Gain in SNR_{myo} from TOF measured in the myocardium of 13 patients plotted against weight and BMI.

the system used, this should facilitate an approximate 25% reduction in the administered activity.

Acknowledgements

The authors wish to extend their thanks to colleagues Kimberley Saint and Matthew Memmott for conscientious proof reading of this manuscript prior to submission.

Disclosure

There are no conflicts of interest for Ian Armstrong, Christine Tonge, and Parthiban Arumugam associated with this study.

References

1. Conti M, Bendriem B, Casey M, Chen M, Kehren F, Michel C, et al. First experimental results of time-of-flight reconstruction on an LSO PET scanner. Phys Med Biol 2005;50:4507-26.
2. Surti S, Kuhn A, Werner ME, Perkins AE, Kolthammer J, Karp JS. Performance of Philips gemini TF PET/CT scanner with special consideration for its time-of-flight imaging capabilities. J Nucl Med 2007;48:471-80.
3. Budinger TF. Time-of-flight positron emission tomography: Status relative to conventional PET. J Nucl Med 1983;24:73-8.
4. Kadrmas DJ, Casey ME, Conti M, Jakoby BW, Lois C, Townsend DW. Impact of time-of-flight on PET tumor detection. J Nucl Med 2009;50:1315-23.

5. Kadrmas DJ, Oktay MB, Casey ME, Hamill JJ. Effect of scan time on oncologic lesion detection in whole-body PET. IEEE Trans Nucl Sci 2012;59:1940-7.
6. Armstrong IS, James JM, Williams HA, Kelly MD, Matthews JC. The assessment of time-of-flight on image quality and quantification with reduced administered activity and scan times in 18F-FDG PET. Nucl Med Commun 2015;36:728-37.
7. DiFilippo FP, Brunken RC. Impact of time-of-flight reconstruction on cardiac PET images of obese patients. Clin Nucl Med 2017;42:e103-8.
8. Oldan JD, Shah SN, Brunken RC, DiFilippo FP, Obuchowski NA, Bolen MA. Do myocardial PET–MR and PET–CT FDG images provide comparable information? J Nucl Cardiol 2016;23:1102-9.
9. Conti M, Eriksson L, Westerwoudt V. Estimating image quality for future generations of TOF PET scanners. 2011 nuclear science symposium conference record (NSS/MIC); 2011:2407-2414
10. Akamatsu G, Ishikawa K, Mitsumoto K, Taniguchi T, Ohya N, Baba S, et al. Improvement in PET/CT image quality with a combination of point-spread function and time-of-flight in relation to reconstruction parameters. J Nucl Med 2012;53:1716-22.
11. Lois C, Jakoby BW, Long MJ, Hubner KF, Barker DW, Casey ME, et al. An assessment of the impact of incorporating time-of-flight information into clinical PET/CT imaging. J Nucl Med 2010;51:237-45.
12. McDermott G, Chowdhury F, Scarsbrook A. Evaluation of noise equivalent count parameters as indicators of adult whole-body FDG-PET image quality. Ann Nucl Med 2013;27:855-61.
13. Yu M, Nekolla SG, Schwaiger M, Robinson SP. The next generation of cardiac positron emission tomography imaging agents: Discovery of flurpiridaz F-18 for detection of coronary disease. Semin Nucl Med 2011;41:305-13.
14. Berman DS, Maddahi J, Tamarappoo BK, Czernin J, Taillefer R, Udelson JE, et al. Phase II safety and clinical comparison with single-photon emission computed tomography myocardial perfusion imaging for detection of coronary artery disease. J Am Coll Cardiol 2013;61:469-77.
15. Cerqueira MD, Allman KC, Ficaro EP, Hansen CL, Nichols KJ, Thompson RC, et al. Recommendations for reducing radiation exposure in myocardial perfusion imaging. J Nucl Cardiol 2010;17:709-18.
16. Dorbala S, Blankstein R, Skali H, Park MA, Fantony J, Mauceri C, et al. Approaches to reducing radiation dose from radionuclide myocardial perfusion imaging. J Nucl Med 2015;56:592-9.
17. Jakoby BW, Bercier Y, Conti M, Bendriem B, Townsend D. Physical and clinical performance of the mCT time-of-flight PET/CT scanner. Phys Med Biol 2011;56:2375-89.
18. Schmidtlein CR, Beattie NJ, Bailey DL, Akhurst TJ, Wang W, Gonen M, et al. Using an external gating signal to estimate noise in PET with an emphasis on tracer avid tumors. Phys Med Biol 2010;55:6299-326.
19. Levin CS, Maramraju SH, Khalighi MM, Deller TW, Delso G, Jansen F. Design features and mutual compatibility studies of the time-of-flight PET capable GE SIGNA PET/MR system. IEEE Trans Med Imaging 2016;35:1907-14.
20. Queiroz MA, Delso G, Wollenweber S, Deller T, Zeimpekis K, Huellner M, et al. Dose optimization in TOF-PET/MR compared to TOF-PET/CT. PLoS ONE 2015;10:e0128842.